Establishment of extrahepatic bile duct cancer organoids using suspension culture and their application in clinical drug screening

WEI HUANG[1*], YUANHUI SU[1*], CHENG YU[1], YANLONG ZHANG[2], HAO XU[3,4] and WENCE ZHOU[1,5]

[1]General Surgery Department, The Second Hospital & Clinical Medical School, Lanzhou University, Lanzhou, Gansu 730000, P.R. China; [2]Pathology Department, Dingxi People's Hospital, Dingxi, Gansu 743000, P.R. China; [3]Department of Hepatobiliary Surgery, The First Affiliated Hospital of Zhejiang Chinese Medical University, Zhejiang Provincial Hospital of Chinese Medicine, Hangzhou, Zhejiang 310006, P.R. China; [4]Hepatobiliary and Pancreatic Surgery Department, The First School of Clinical Medicine, Zhejiang Chinese Medical University, Hangzhou, Zhejiang 310006, P.R. China; [5]Department of General Surgery, Lanzhou University Second Hospital, Lanzhou, Gansu 730000, P.R. China

Received January 29, 2026; Accepted April 2, 2026

DOI: 10.3892/ol.2026.15770

Abstract. The present study aims to explore the feasibility of establishing human extrahepatic cholangiocarcinoma (eCCA) organoids via suspension culture, to biologically characterize their biological features and to evaluate their drug sensitivity, thereby providing a preclinical model for personalized precision therapy. Surgically resected tumor tissues were obtained from patients with eCCA. Tumor cells were isolated by mechanical dissociation and enzymatic digestion, and were cultured in a matrix-free suspension system for three-dimensional organoid formation and continuous passaging. Histomorphological features of the organoids and the corresponding parental tumor tissues were compared by H&E staining. Immunohistochemistry was used to detect the expression of the cholangiocyte markers cytokeratin (CK)7 and CK19, as well as Ki-67, to confirm tissue origin and proliferative activity. In addition, the organoid model was used for *in vitro* sensitivity testing of conventional chemotherapy regimens. The organoids exhibited morphological features of moderately to poorly differentiated adenocarcinoma, consistent with those of the parental tumors, including tubular structures, solid nests and nuclear atypia. Immunohistochemical analysis showed high expression of CK7 and CK19, confirming cholangiocytic origin, along with high Ki-67 expression, indicating active proliferative capacity. Drug sensitivity testing revealed substantial heterogeneity in treatment responses among organoid lines derived from different patients, indicating variable sensitivity to chemotherapeutic agents. In conclusion, an eCCA organoid model was successfully established using a suspension culture method, and it largely preserved the histopathological and cellular phenotypic features of the parental tumor. This model functions as an *in vitro* 'patient surrogate' for drug-sensitivity testing, with potential for evaluating chemotherapy and targeted-drug efficacy. However, the observed clinical concordance in a single patient is preliminary and its definitive predictive value requires validation in larger prospective cohorts. Theoretically, this system offers advantages in scalability and standardization for clinical applications, although direct comparisons with traditional matrices remain to be conducted.

Correspondence to: Dr Hao Xu, Hepatobiliary and Pancreatic Surgery Department, The First School of Clinical Medicine, Zhejiang Chinese Medical University, 54 Youdian Road, Shangcheng, Hangzhou, Zhejiang 310006, P.R. China
E-mail: amoyxu@126.com

Dr Wence Zhou, Department of General Surgery, Lanzhou University Second Hospital, 82 Cuiyingmen, Chengguan, Lanzhou, Gansu 730000, P.R. China
E-mail: zhouwc129@163.com

*Contributed equally

Key words: extrahepatic cholangiocarcinoma, organoids, precision medicine, establishment, characterization

Introduction

Cholangiocarcinoma (CCA) is a highly heterogeneous epithelial carcinoma with variable degrees of differentiation (1,2). Based on anatomical location, CCA is classified into intrahepatic CCA and extrahepatic cholangiocarcinoma (eCCA). According to the location relative to the cystic duct, eCCA is further subdivided into perihilar cholangiocarcinoma and distal cholangiocarcinoma (3,4). eCCA accounts for 20-30% of all biliary tract cancers (5). Established risk factors mainly include non-alcoholic fatty liver disease, liver cirrhosis and primary sclerosing cholangitis (6). Over recent decades, the incidence of eCCA has increased steadily. However, the prognosis remains poor, with a 5-year survival rate of ~11% (7,8). Surgery is still the only curative treatment for non-metastatic eCCA. For patients with advanced disease, the primary treatment strategy is chemotherapy combined with immunotherapy,

although the therapeutic efficacy remains limited. Therefore, investigation of the pathogenesis of eCCA and development of more effective therapies are of great importance.

Unlike tumor cell lines, organoids are three-dimensional (3D) structures derived from pluripotent stem cells or isolated organ progenitor cells. These structures can self-organize into 'mini-organs' that recapitulate the architecture of native tissues (9) and reproduce the pathophysiological characteristics of the parental tumors (10). Organoids closely mimic the structure and function of primary tissues while retaining high genetic fidelity and donor-specific therapeutic responses (11). Furthermore, the establishment of organoids requires substantially less time and tissue than the generation of patient-derived xenograft models (12). Importantly, compared to animal-based models, organoid systems offer a significant ethical advantage by reducing or replacing the need for animal experimentation, thereby addressing animal welfare concerns. While the use of human-derived cells for *in vitro* culture involves its own distinct ethical considerations, it bypasses many of the complex ethical implications inherent in animal testing.

This study aimed to explore the feasibility of establishing eCCA organoids using suspension culture, with the goal of providing a potentially more economical and rapid alternative construction platform for basic research on this malignancy.

Materials and methods

Tissue sources. For organoid culture, tumor tissues were collected from five patients with a preoperative diagnosis of eCCA who underwent surgical resection at the Second Hospital of Lanzhou University (Lanzhou, China) between February 2023 and December 2024. These tissues were used to establish patient-derived organoid models. None of the patients had received radiotherapy or chemotherapy before surgery. This study was conducted in accordance with the Declaration of Helsinki. The study protocol was approved by the Ethics Committee of the Second Hospital of Lanzhou University (approval no. 2023A-381) and informed consent was obtained from all patients and/or their legal guardians, as appropriate.

Primary reagents, instruments and consumables. DMEM/F12 medium, trypsin and fetal bovine serum were purchased from Biological Industries. GlutaMAX and Dispase II were from Invitrogen (Thermo Fisher Scientific, Inc.). Collagenase II was purchased from Gibco (Thermo Fisher Scientific, Inc.). Serum-free cell cryopreservation medium was obtained from NCM Biotechnology Co., Ltd. Antibodies against cytokeratin (CK)7 (cat. no. MAB-0828; dilution, 1:100), CK19 (cat. no. MAB-0829; dilution, 1:100) and Ki-67 (cat. no. RMA-0542; dilution, 1:100) were purchased from Fuzhou Maixin Biotechnology Co., Ltd. The horseradish peroxidase-conjugated universal secondary antibody (cat. no. KIT-5020) was purchased from Fuzhou Maixin Biotechnology Co., Ltd. Penicillin-streptomycin solution and penicillin-streptomycin-amphotericin B solution were obtained from Shanghai Dotehill Biological Technology Co., Ltd. PBS was purchased from Wuhan Servicebio Technology Co., Ltd. Gemcitabine hydrochloride for injection was obtained from Jiangsu Hansoh Pharmaceutical Group Co., Ltd., Oxaliplatin for injection from Jiangsu Hengrui Pharmaceuticals Co., Ltd., 5-Fluorouracil (5-FU) injection from Shanghai Xudong Haipu Pharmaceutical Co., Ltd. and albumin-bound paclitaxel from Wuxi Zishan Pharmaceutical Co., Ltd.

The major instruments used in this study included an inverted microscope (Nikon Corp.) and a paraffin microtome (Leica Microsystems GmbH).

Primary consumables included ultra-low attachment plates, 50-ml centrifuge tubes, 1,000-μl pipette tips, pasteur pipettes and 60-mm culture dishes purchased from NEST Biotechnology Co., Ltd. Furthermore, 15-ml centrifuge tubes and microcentrifuge tubes were obtained from Wuhan Servicebio Technology Co., Ltd.

Establishment of organoid models. Fresh tumor tissues were collected under aseptic conditions and processed as follows. The organoid culture protocol was established based on our previously described method with minor modifications (13). A tissue block of ~1x1x1 cm was excised for organoid culture and placed in a 15-ml centrifuge tube containing 10 ml of transport medium, namely complete organoid culture medium consisting of DMEM/F12 supplemented with 1X GlutaMAX, 10% fetal bovine serum and 1% penicillin-streptomycin solution. In addition, a tumor tissue fragment measuring ~0.5x0.5x0.5 cm was placed in a 2-ml microcentrifuge tube and stored at -80˚C for subsequent experiments. The centrifuge tube was immediately transported to the laboratory in a specimen transport box containing crushed ice.

Upon arrival at the laboratory, the tumor tissue was transferred to a 60-mm culture dish and rinsed with 5 ml of PBS to remove blood clots and necrotic debris. The tissue was then carefully minced with a sterile No. 23 surgical scalpel. Subsequently, 5 ml of mixed digestive enzyme solution (consisting of Collagenase II at 1 mg/ml and Dispase II at 2 mg/ml in DMEM/F12) was added at room temperature and the resulting tissue suspension was transferred into a 15-ml centrifuge tube using a Pasteur pipette. The tube was placed on a shaker and digested at 37˚C for ~45 min. During this period, the digestion process was closely monitored. When the tissue volume had decreased by approximately half, the tube was allowed to stand undisturbed for 10 min. The supernatant was then carefully transferred into a new centrifuge tube using a Pasteur pipette and centrifuged at 150 x g for 5 min at 4˚C. After removal of the supernatant, this washing step was repeated twice to remove residual digestive enzymes and cellular debris. The final pellet was resuspended in complete organoid culture medium consisting of DMEM/F12 supplemented with 1X GlutaMAX, 10% fetal bovine serum and 1% penicillin-streptomycin solution. The cell suspension was then evenly seeded into a 12-well ultra-low-attachment plate, and the volume in each well was adjusted to 3 ml with complete organoid culture medium, to initiate organoid culture. The cells were cultured at 37˚C in a 5% CO_2 humidified incubator. Visible cell aggregates typically formed within 2-3 days, and organoids reached ~100 μm in diameter within 5-7 days after seeding.

Passaging, freezing and thawing of organoids

Passaging. During organoid culture, the morphology of organoids in each well was photographed every 2 days. Passaging

was performed when the diameter of the eCCA organoids reached ~100 μm. The organoid suspension from each well was collected into a 50-ml centrifuge tube using a Pasteur pipette. Approximately 10 ml of PBS was added and the suspension was gently mixed by pipetting with a 1,000-μl pipette tip, followed by centrifugation at 340 x g for 5 min at 4˚C. The supernatant was discarded. Next, 3 ml of 0.25% trypsin was added to the organoid pellet and mixed gently. Digestion was carried out at 37˚C and monitored under a light microscope using a 4x objective lens (total magnification, x40). When the organoid clusters had dissociated into small fragments containing <10 cells, digestion was terminated by adding 6 ml of complete organoid medium. The suspension was gently pipetted again with a 1,000-μl pipette tip, then centrifuged at 340 x g for 5 min at 4˚C, and the supernatant was removed. For passaging at a split ratio of 1:2 to 1:3, 12 ml of complete organoid medium was added to the centrifuge tube and the pellet was gently resuspended. Subsequently, one-half or one-third of the organoid suspension was evenly seeded into a new 12-well ultra-low attachment plate and the volume in each well was adjusted to 3 ml with complete medium. Culture was subsequently continued as described above.

Cryopreservation. The remaining organoids in the centrifuge tube were centrifuged at 340 x g for 5 min at 4˚C. According to the pellet size, 1-2 ml of cryopreservation medium was added and the pellet was gently resuspended by pipetting. A commercial cell-freezing medium was also acceptable. The suspension was then transferred to a 2-ml cryovial and stored in liquid nitrogen for long-term preservation.

Thawing. For organoid recovery, the cryovial was rapidly thawed in a 37˚C water bath. The organoid suspension was then immediately transferred to a 15-ml centrifuge tube using a 1,000-μl pipette tip. Next, 5 ml of complete organoid culture medium was added and the suspension was gently mixed by pipetting. After centrifugation at 340 x g for 5 min at 4˚C, the supernatant was discarded. The pellet was then resuspended in 12 ml of complete organoid culture medium, gently mixed again and evenly seeded into a 12-well ultra-low-attachment plate. Organoid culture was continued as described above.

Organoid embedding and sectioning. After centrifugation of the organoid suspension at 340 x g at 4˚C for 5 min, 5 ml of 4% paraformaldehyde fixative was added to the centrifuge tube and fixation was carried out at 37˚C for 24 h. The samples were then dehydrated through a graded ethanol series (50, 70, 80, 95 and 100% x2), with each step lasting 30 min. Subsequently, the fixed organoid blocks were immersed in a xylene-ethanol mixture (1:1) for 30 min, followed by two incubations in pure xylene for 1 h each. The organoid blocks were then embedded in paraffin and the paraffin blocks were sectioned into slices ~5 μm thick using a microtome. The sections were mounted on glass slides, air-dried and stored for subsequent use.

Hematoxylin and eosin (H&E) staining of organoids and primary tumor tissue. Sections from paraffin-embedded organoid blocks and primary tumor tissue blocks were mounted on glass slides and placed on staining racks. Deparaffinization was performed in xylene (3x2 min), followed by rehydration through a graded ethanol series consisting of 100% ethanol (3x2 min), 95% ethanol (2 min) and 70% ethanol (2 min). The slides were then rinsed under running tap water at room temperature for at least 5 min.

Staining was performed with eosin solution for 2 min, followed by differentiation in 95% ethanol with ~20 dips. The sections were then dehydrated sequentially in 95% ethanol for 2 min and 100% ethanol (2x2 min). Clearing was performed in xylene (3x2 min). Finally, the sections were mounted with neutral balsam and covered with coverslips. Slides that passed microscopic quality control were subjected to image acquisition and analysis.

Immunohistochemistry of organoids. Cryopreserved eCCA tumor tissues stored at -80˚C were fixed in 4% paraformaldehyde and embedded in paraffin to prepare 5 μm-thick sections, following the protocol previously described for organoids. To characterize the tissue origin and proliferative activity, both organoid sections and tumor tissue sections were subjected to standard chromogenic immunohistochemistry. After deparaffinization and rehydration through a graded ethanol series, antigen retrieval was performed in citrate buffer using a microwave oven, and endogenous peroxidase activity was blocked with 3% H_2O_2. The sections were then incubated overnight at 4˚C with primary antibodies against CK7, CK19 and Ki-67, each at a dilution of 1:100. On the following day, a horseradish peroxidase-conjugated universal secondary antibody (ready-to-use) was applied for 30 min at room temperature, followed by visualization with 3,3'-diaminobenzidine. Positive signals were identified as brownish-yellow precipitates under a light microscope. Finally, the slides were counterstained with hematoxylin and mounted. Image acquisition and analysis were performed using optical microscopy. For Ki-67 quantification, two pathologists independently and blindly evaluated five randomly selected high-power fields per slide using ImageJ software (version 1.54f; National Institutes of Health). The mean percentage of positive nuclei relative to the total cell count was then calculated to determine the final labeling index.

Drug sensitivity testing of organoids. Organoids were collected into a 15-ml centrifuge tube using a Pasteur pipette, centrifuged at 97 x g for 5 min at room temperature and the supernatant was discarded. The organoid pellet was then digested with trypsin to obtain a single-cell suspension. After cell counting with a hemocytometer, 100 μl of cell suspension adjusted to a cell density of $1.2x10^5$ cells/ml was evenly added into each well of a 96-well plate (NEST Biotechnology Co., Ltd). After 24 h, four antitumor drugs, gemcitabine, oxaliplatin, 5-FU and albumin-bound paclitaxel, were diluted in complete medium (RPMI-1640 supplemented with 10% fetal bovine serum and 1% penicillin-streptomycin) to the following concentrations. These concentration ranges were established based on our preliminary dose-finding experiments. Gemcitabine (600, 150, 30, 6, 1.5, 0.3, 0.06, 0.015, 0.003, 0.0006, 0.00015, 0.00003, 0.000006 and 0.0000012 μmol/l), oxaliplatin (400, 200, 100, 40, 20, 10, 5, 2.5, 1.25, 0.625, 0.3125, 0.15625, 0.078 and 0.039 μmol/l), 5-FU (7,680, 1,920, 384, 96, 24, 6, 1.5, 0.3, 0.06, 0.015, 0.003, 0.0006, 0.00015 and 0.00003 μmol/l) and albumin-bound paclitaxel (40, 20, 10, 5, 2.5, 0.5, 0.1, 0.025, 0.005, 0.001, 0.00025, 0.00005, 0.00001 and 0.0000025 μmol/l). After removal of

Table I. Clinical data of 5 patients with cholangiocarcinoma.

Parameter	Patient 1	Patient 2	Patient 3	Patient 4	Patient 5
Age, years	58	58	66	68	61
Sex	Male	Male	Female	Male	Female
Diagnosis date	2023/02	2023/04	2023/08	2024/12	2024/01
Survival status	Alive	Alive	Alive	Alive	Alive
Sample site	Distal CBD	Mid CBD	Mid CBD	Mid CBD	Proximal CBD
Tumor size, mm	30x20	20x15	-	20x18	35x30
TNM	T2N1M0	T1N0M0	T2N0M0	T2N0M0	T3N1M0
Tumor differentiation	Moderately differentiated	Poorly differentiated	Moderately differentiated	Moderately differentiated	Moderately-poorly differentiated
CEA, ng/ml	2.8	0.54	2.97	0.95	1.15
CA19-9, ng/ml	344	36	327	890	91

Patient survival data cutoff: October 1, 2025. CEA, carcinoembryonic antigen; CA19-9, carbohydrate antigen 19-9; CBD, common bile duct.

the spent medium, 170 μl of the corresponding drug solution was added to each well. The plate included a control group and drug treatment groups. The control group received 170 μl of complete medium, whereas the treatment groups received an equal volume of the corresponding drug solution. The control group and each drug concentration group were set up in quadruplicate. After 72 h of culture, the medium was removed and 100 μl of Cell Counting Kit (CCK)-8 (APExBIO Technology LLC) diluted in RPMI-1640 at a 1:9 ratio was added to each well. Following incubation at 37˚C for 3 h, the absorbance at 450 nm was measured using a microplate reader (Synergy H1; Biotek China). The experiment was independently performed in quadruplicate. Drug dose-response curves were generated and the half-maximal inhibitory concentration (IC_{50}) values were calculated using GraphPad Prism software, version 9.5.1 (Dotmatics). IC_{50} values were determined by a nonlinear regression using the following four-parameter logistic equation:

$$Y = Bottom + \frac{Top - Bottom}{1 + 10^{(LogIC_{50} - X) \cdot HillSlope}}$$

where X is the logarithm of the drug concentration, Y is the normalized cell viability and HillSlope represents the slope of the dose-response curve. In the four-parameter logistic equation, Top represents the maximum response (cell viability at the lowest drug concentration, typically approaching 100% viability) and Bottom represents the minimum response (cell viability at the highest drug concentration, where inhibition reaches a plateau).

Results

Establishment of extrahepatic bile duct cancer organoids. A total of five eCCA tumor tissue samples were collected in this study and the clinical data of the patients are summarized in Table I. Tumor samples were obtained from five patients (age range: 58-68 years; median age: 61 years; three males and two females), and three organoid lines were successfully established, yielding an overall success rate of 60%. These were designated as Organoid-P1, Organoid-P2 and Organoid-P3, which were derived from Patient 1, Patient 2 and Patient 5, respectively, as listed in Table I (numbered sequentially according to successful establishment).

The two unsuccessful cases were mainly attributed to low initial cell viability and marked tissue necrosis in the surgical specimens. After serial passaging, cryopreservation and thawing, stable eCCA organoids were successfully maintained without a significant reduction in viability. Under an inverted microscope, the organoids exhibited irregular cystic, grape-like, lobulated or solid morphologies. Some organoids retained central luminal structures resembling biliary duct-like cavities, with heterogeneous cyst sizes and irregular shapes (Fig. 1).

H&E staining results of eCCA organoids and primary tumor tissue. H&E staining was performed to evaluate the histomorphological features of the established eCCA organoids. The results showed that the organoids exhibited cystic or irregular gland-like structures, accompanied by marked nuclear atypia and pathological mitotic figures (Fig. 2). These features closely resembled the histoarchitectural characteristics of the corresponding primary tumor tissues.

Immunohistochemical findings in eCCA organoids. The protein expression levels of CK19, CK7 and Ki-67 in eCCA organoids were assessed by immunohistochemistry. The results showed strong positive expression of CK7 and CK19 in all organoid lines. This robust and uniform expression pattern further supports the high fidelity of the organoids to the biliary epithelial origin of the primary tumors. Positive staining was mainly localized to the cytoplasm and cell membrane and showed a homogeneous distribution throughout the organoid architecture. Quantitative analysis based on double-blind counting in five randomly selected high-power fields showed that all three organoid lines maintained high proliferative activity. Specifically, the Ki-67 labeling indices were 30.0±1.9% for Organoid-P1, 39.5±1.4% for Organoid-P2 and 40.3±1.1% for Organoid-P3 (Fig. 3).

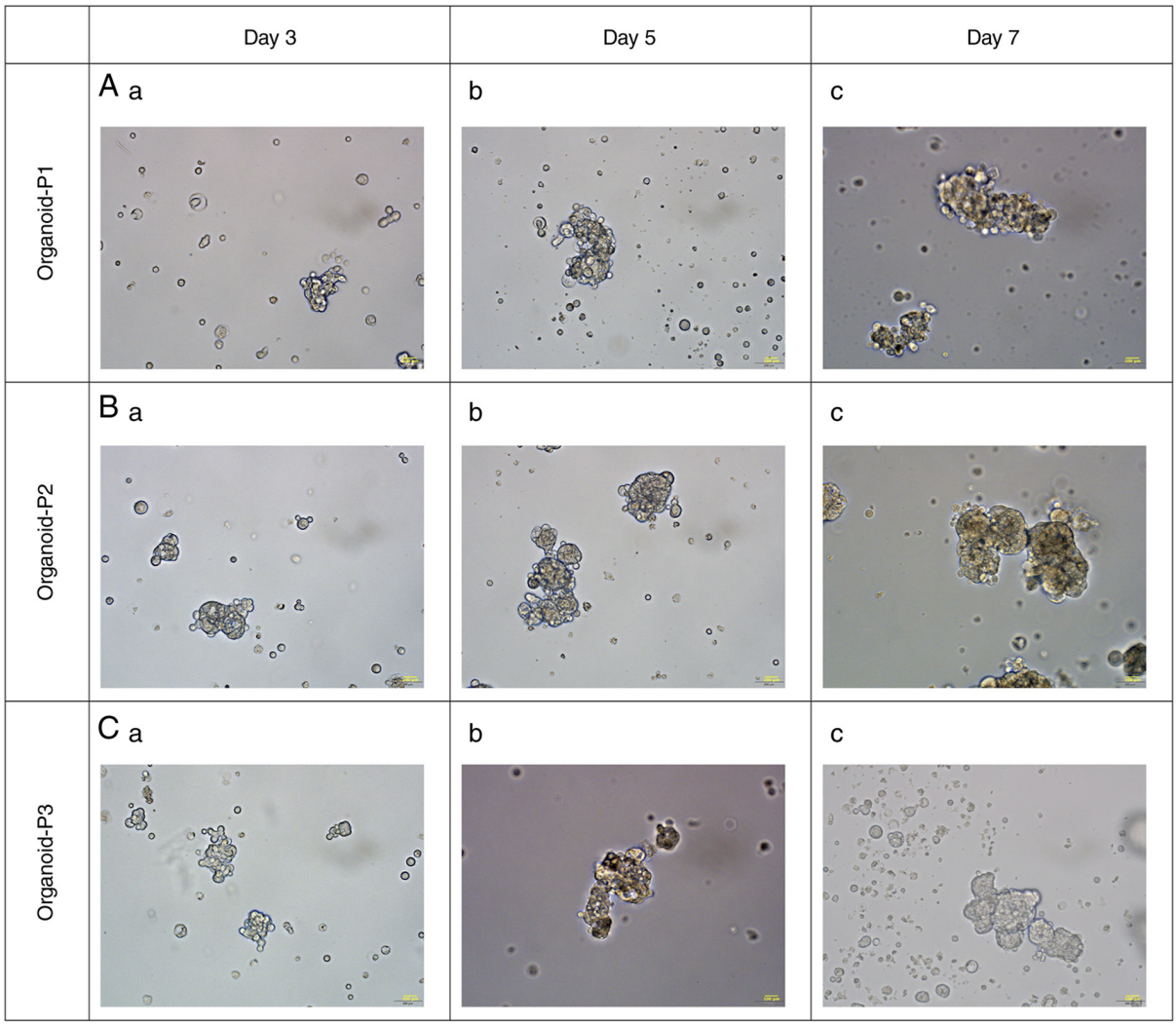

Figure 1. Representative microscopic images of extrahepatic cholangiocarcinoma organoids. (A-C) Morphological evolution of three independent extrahepatic cholangiocarcinoma organoid lines at passage 3 from day 3 to day 7. (A) Organoid-P1, (B) Organoid-P2 and (C) Organoid-P3. In each panel, (a-c) indicate images captured on (a) day 3, (b) day 5 and (c) day 7 after passaging. The organoids exhibited irregular cystic, grape-like, lobulated, or solid morphologies, with some organoids retaining central luminal structures resembling biliary duct-like cavities (magnification, x200; scale bars, 100 μm).

Drug sensitivity testing and screening of eCCA organoids. The drug-sensitivity testing results for Organoid-P1 (Fig. 4) showed differential responses to gemcitabine, 5-FU, albumin-bound paclitaxel and oxaliplatin. Organoid-P1 was sensitive to gemcitabine (IC_{50}=0.1978±0.0331 μmol/l), 5-FU [IC_{50}=(7.57±1.10) x 10^{-2} μmol/l] and albumin-bound paclitaxel [IC_{50}=(8.09±1.50) x 10^{-4} μmol/l], but was resistant to oxaliplatin (IC_{50}=331.8±73.1 μmol/l). Patient 1, from whom Organoid-P1 was derived, received seven cycles of postoperative combination therapy with gemcitabine, tegafur-gimeracil-oteracil (S-1) and sintilimab. Regular follow-up examinations, including serial measurements of serum tumor markers (AFP, CEA, CA19-9 and CA-125) at different postoperative time-points (Fig. 5), showed no evidence of tumor recurrence within 12 months after surgery. These findings provide clinical support for the feasibility and predictive value of the organoid-based drug-sensitivity testing platform. It should be noted that comprehensive drug sensitivity testing was performed only on Organoid-P1, as the primary goal of this study was to provide proof-of-concept validation by comparing *in vitro* drug responses with actual clinical outcomes. Patient 1 had complete follow-up data and received standard postoperative chemotherapy, making Organoid-P1 the appropriate line for establishing clinical concordance.

Discussion

In the present study, a human eCCA organoid culture system was successfully established using suspension culture and its potential for clinical drug screening was preliminarily validated. These findings provide a novel research model and suggest a new direction for personalized therapy in this highly aggressive malignancy with a poor prognosis. Although the conventional Matrigel-based method remains the standard approach, batch-to-batch variability associated with its animal-derived origin may compromise reproducibility. In theory, the matrix-free approach used here may offer advantages in scalability and cost-effectiveness (14). It should be clarified that while the present study is not the first to establish CCA organoids, as Matrigel-based models for both

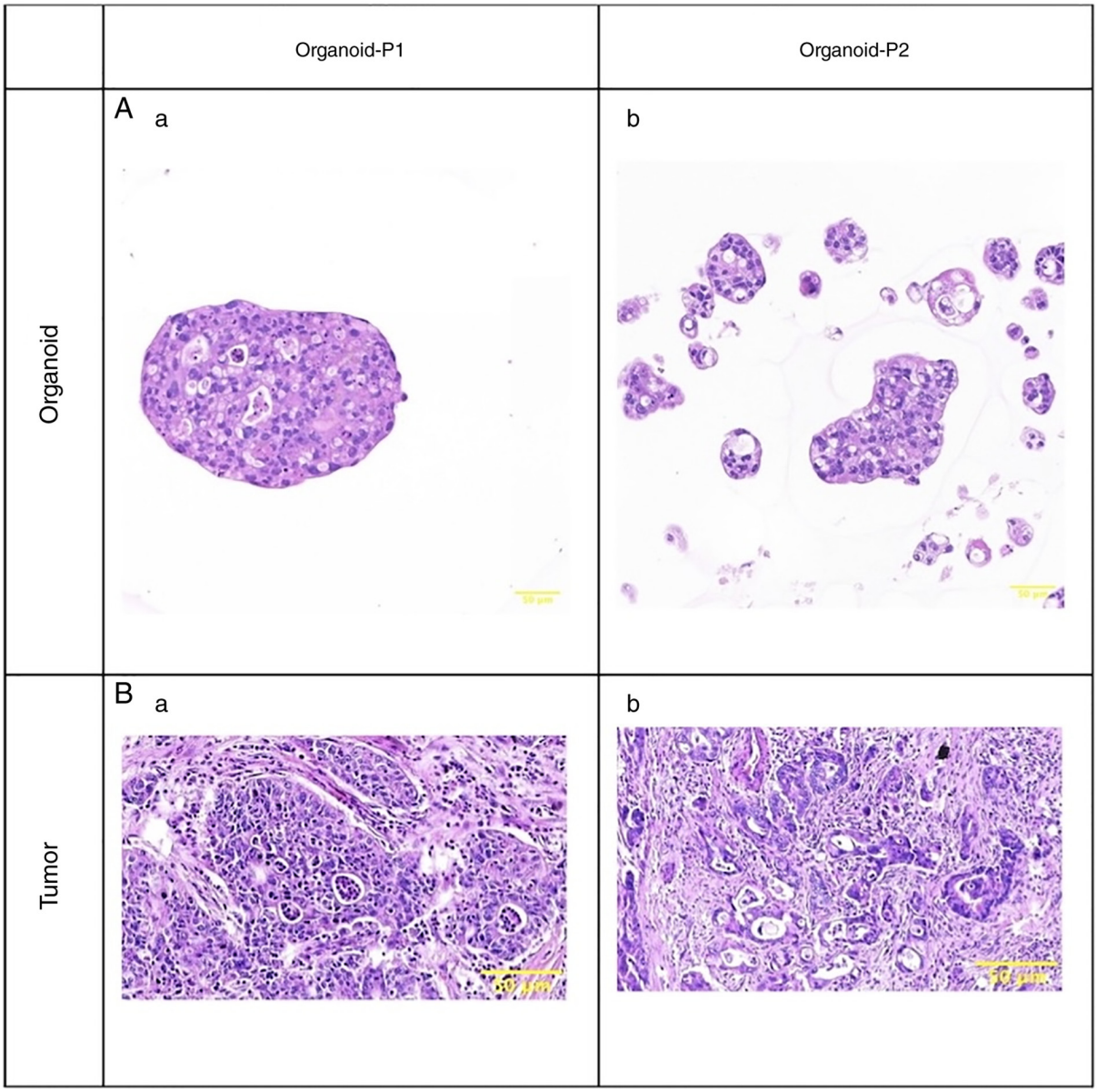

Figure 2. Histomorphological comparison between organoids and parental tissues. H&E staining of two representative extrahepatic cholangiocarcinoma organoid lines (passage 5) and their corresponding primary tumor tissues. (A) Organoid-P1 and its matched parental tumor tissue. (B) Organoid-P2 and its matched parental tumor tissue. In each panel, (a) indicates the organoid, whereas (b) indicates the corresponding parental tumor tissue. The organoids retained key histological features of the parental tumors, including irregular gland-like structures, nuclear atypia and glandular architectural characteristics (magnification, x200; scale bars, 50 μm).

intrahepatic and extrahepatic CCA have been described previously (15), it represents a novel implementation of a matrix-free suspension culture system specifically optimized for human eCCA. Currently, organoid technology is a rapidly advancing field and has been successfully established and utilized as 'patient surrogates' for various malignancies beyond eCCA, including gastric cancer (13), primary liver cancer (16) and lung cancer (17), demonstrating its robust predictive value for clinical drug responses.

In the present study, H&E staining confirmed that suspension-cultured CCA organoids retained the histological architecture of the primary tumors, as well as the characteristic strong cytoplasmic expression of biliary markers (CK7 and CK19). This high degree of resemblance may underlie the potential clinical relevance of the experimental findings and supports the use of these organoids as a promising alternative platform for drug screening. Previous work by our research group successfully established gastric cancer organoids using suspension culture, and these organoids closely resembled the original tissues and served as effective models for personalized drug screening (13). In addition, the matrix-free suspension culture strategy adopted in the present study was based on previous work on hepatic ductal organoids, in which efficient organoid expansion was achieved using stirred-tank bioreactors (18). Furthermore, a recent study on polyisocyanopeptide-based hydrogel functionalized with invasin hydrogel have shown that it can support the long-term three-dimensional expansion of various epithelial organoids, with efficacy comparable to that of Matrigel (19). Collectively, these studies help reduce reliance on complex natural matrices

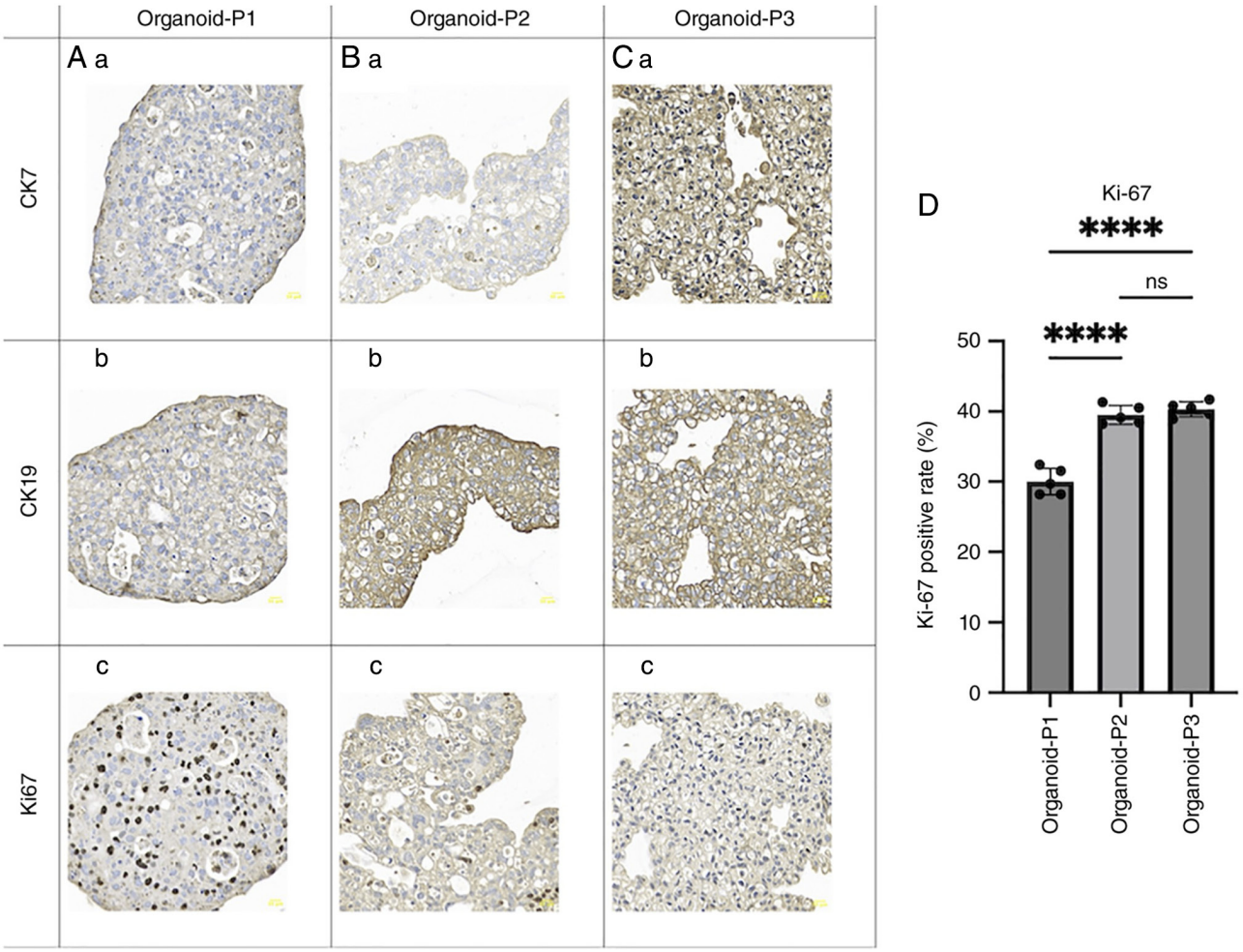

Figure 3. Immunohistochemical expression of biliary markers and Ki-67. Staining for (a) CK7, (b) CK19 and (c) Ki-67 in (A) organoid-P1, (B) organoid-P2 and (C) organoid-P3. (D) Quantitative analysis of Ki-67 labeling indices (mean ± SD) based on blinded counting of five random high-power fields. Images were captured at a total magnification of x200 (scale bar, 50 μm). ****P<0.0001. ns, no significance; CK, cytokeratin.

and promote the development of chemically defined and scalable organoid culture systems.

In the context of precision medicine, drug sensitivity testing using eCCA organoids show considerable potential for advancing personalized therapy. Organoids derived from different patients exhibit markedly different responses to standard chemotherapy regimens, such as gemcitabine/cisplatin, and these differences are closely associated with actual clinical outcomes (16). This suggests that prospective drug screening using patient-derived organoids before treatment initiation may help identify effective therapeutic strategies while avoiding the toxicity and treatment delays associated with ineffective therapies (16,17). This approach is particularly valuable for patients with eCCA, who usually face limited treatment options and poor outcomes. Conventional two-dimensional cell lines are often limited by low culture success rates. In addition, they are prone to genetic drift and loss of heterogeneity during *in vitro* passaging, which markedly restricts their predictive value for clinical drug responses (20). Multiple prospective clinical studies have reported a high degree of concordance between organoid drug sensitivity and patient outcomes, supporting the role of organoids as promising *in vitro* models for personalized medicine. Consistent with these findings, the present study showed that the drug-sensitivity profile of Organoid-P1 was in agreement with the clinical response of patient 1. Notably, Organoid-P1 exhibited marked resistance to oxaliplatin (IC_{50}=331.8±73.1 μmol/l), which is consistent with the clinical selection of the GS regimen (gemcitabine and S-1) rather than an oxaliplatin-based regimen for patient 1. This resistance is also consistent with previous findings showing that a subset of patients with eCCA derives limited benefit from platinum-based therapies, further supporting the utility of organoids in identifying potentially ineffective treatments (21,22). However, despite the high biological fidelity of this model, this single clinical correlation should be interpreted cautiously as preliminary and hypothesis-generating. Validation in larger prospective cohorts is still required to determine the definitive predictive value of this platform in eCCA.

However, the translation of organoid-based drug sensitivity testing into routine clinical practice still faces several challenges. A major limitation of the current model is its simplified composition, as it consists predominantly of tumor epithelial cells and lacks critical components of the tumor microenvironment, such as immune cells and fibroblasts (23). Although Patient 1 showed no recurrence after receiving a

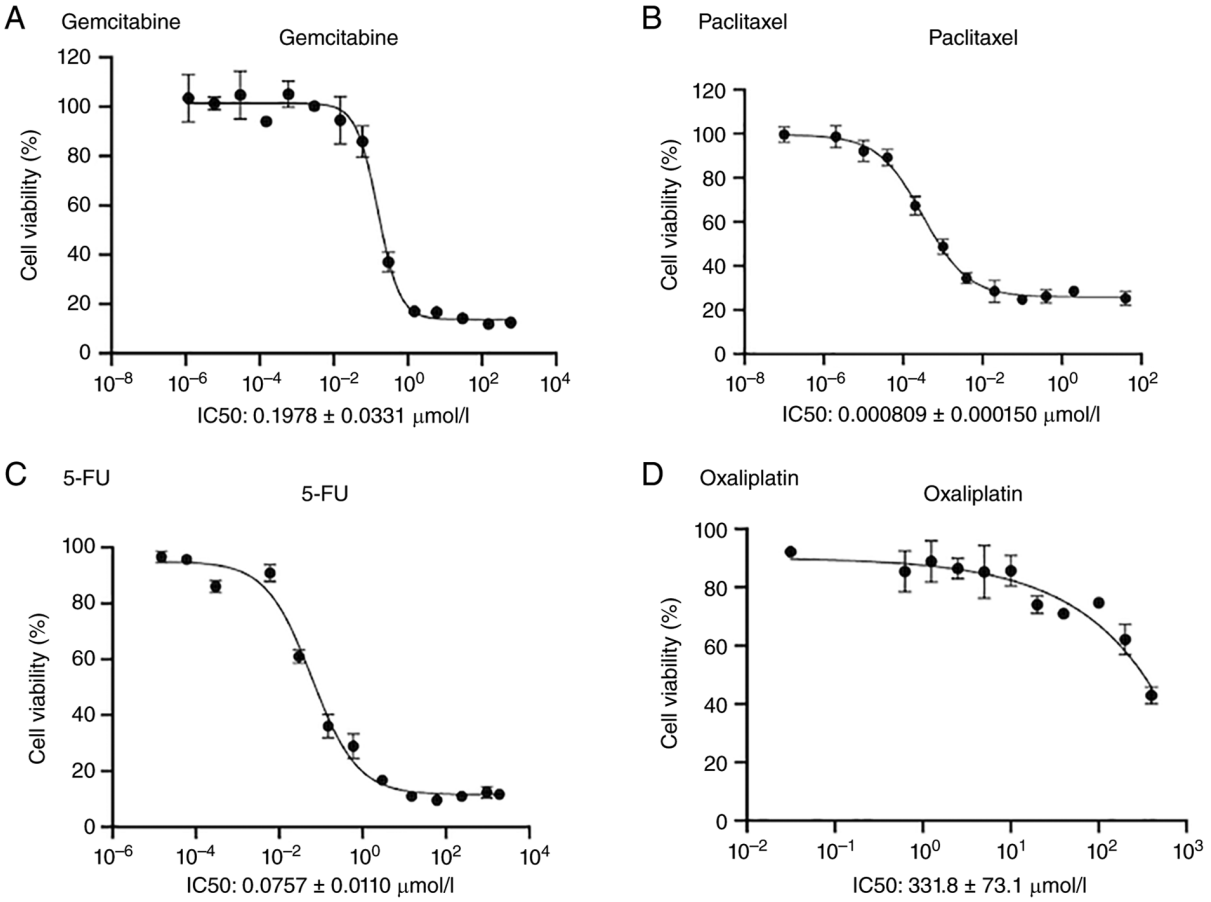

Figure 4. *In vitro* drug sensitivity profiles of organoid-P1. Dose-response curves for (A) Gemcitabine, (B) Nab-paclitaxel, (C) 5-FU and (D) Oxaliplatin. Data are presented as the mean ± SD from four independent biological replicates (n=4), with each drug concentration tested in quadruplicate technical replicates. IC_{50} values were determined using a four-parameter logistic regression model. 5-FU, 5-fluorouracil.

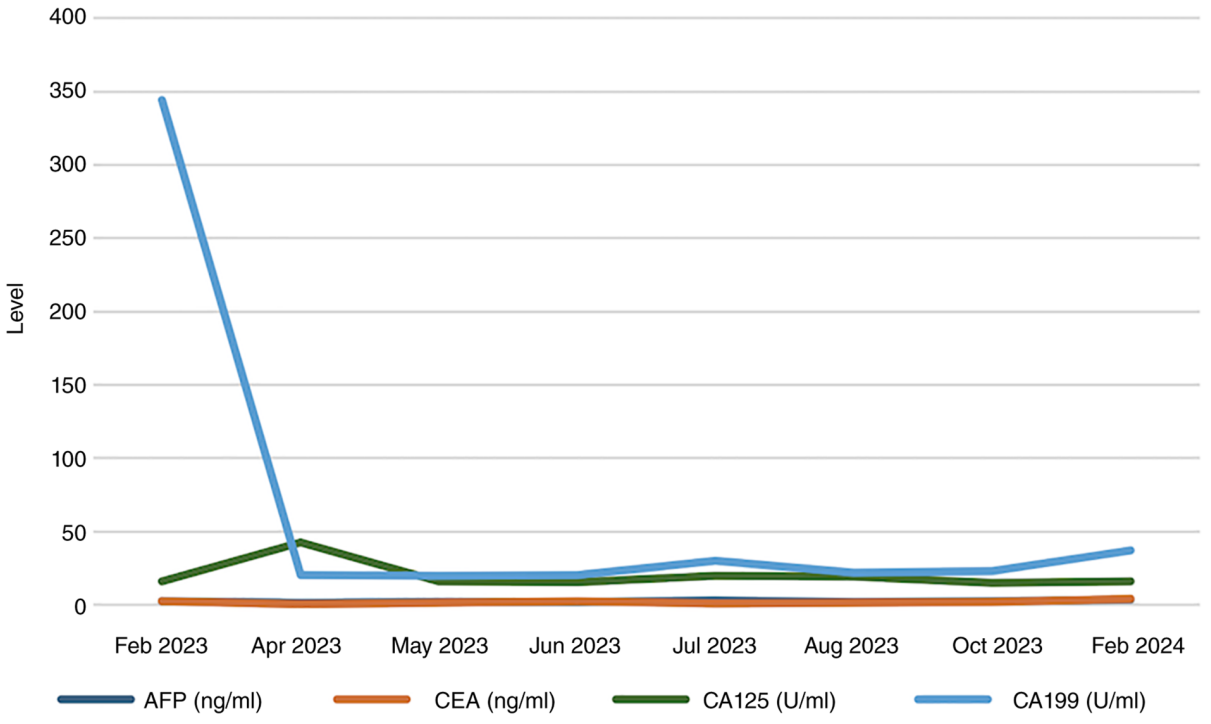

Figure 5. Changes in tumor markers at different time-points after surgery. Patient 1 underwent surgery in March 2023, received 7 cycles of combination chemotherapy with Gemcitabine, Tegafur Gimeracil Oteracil Potassium (S-1) and Sintilimab postoperatively, and has undergone regular follow-up examinations. The x-axis shows the follow-up dates, with only the month and year displayed to preserve patient privacy. No signs of tumor recurrence were detected at 12 months postoperatively. AFP, alpha-fetoprotein; CEA, carcinoembryonic antigen; CA19-9, carbohydrate antigen 19-9; CA-125, carbohydrate antigen 125.

regimen that included the programmed cell death-1 inhibitor sintilimab, the current organoid model, composed solely of tumor epithelial cells, cannot predict or evaluate responses to immunotherapy. Therefore, the favorable clinical outcome observed in this patient may mainly reflect sensitivity to the chemotherapy components, gemcitabine and S-1, rather than immune-mediated effects. Future studies should address this limitation by establishing co-culture systems of organoids with autologous immune cells from patients (24,25) thereby enabling evaluation of the efficacy of immune checkpoint inhibitors (17,26) and facilitating the development of more predictive 'all-in-one' drug sensitivity models. In parallel, the standardization and automation of culture protocols, together with cost reduction, will be essential for large-scale clinical application.

With regard to technical feasibility, the successful establishment rate in this study was 60% (3/5), which reflects the inherent difficulty of organoid culture in biliary tract cancer. The failures in the remaining two cases may be attributable to both biological and technical factors. First, marked intratumoral heterogeneity and differences in the proportion of cancer stem cells may lead to variation in malignant proliferative capacity among samples. Second, the advanced age of the two patients in the failed cases (66 and 68 years) compared to the successful cases (58, 58 and 61 years) may have been associated with reduced cellular proliferative potential. In addition, both failed cases were moderately differentiated tumors, and their relatively lower degree of malignancy and slower proliferative rate, compared to poorly differentiated tissues, may have led to poor adaptation to the matrix-free suspension environment, subsequently promoting apoptosis. From a technical perspective, the high stromal content of these specimens required prolonged enzymatic digestion, which may have reduced primary cell yield and increased cellular damage. Finally, the anatomical proximity of the bile duct to the intestinal lumen increases the risk of microbial contamination. This issue was encountered during the culture process and remains a major obstacle to successful organoid establishment. In future work, the organoid biobank will be expanded by incorporating a broader range of sample types. In addition, the culture process should prioritize the maintenance of cellular viability rather than prolonged culture duration, and the methodology should be further standardized accordingly.

In summary, this study successfully established eCCA organoid models using suspension culture and preliminarily demonstrated their potential for exploring personalized treatment strategies. With continued technical optimization and further clinical validation, suspension-cultured organoids may become a valuable tool for guiding precision therapy in patients with eCCA.

Acknowledgements

Not applicable.

Funding

This study was supported by the National Natural Science Foundation of China (grant no. 82260555), Zhejiang Province Traditional Chinese Medicine Science and Technology Plan Project (grant no. 2025ZL290), Gansu Provincial Top-notch Talent Program [grant no. (2023)9], Cuiying Science and Technology Innovation Project of Lanzhou University Second Hospital (grant no. CY2024-CQ-01), Department of Education of Gansu Province, Excellent Graduate Student 'Star of Innovation' Project (grant no. 2025CXZX-020), Lanzhou University Innovation and Entrepreneurship Cultivation Project (grant no. cxcy2024002) and the Cuiying Scientific Training Program for Undergraduates of the Second Hospital & Clinical Medical School, Lanzhou University (grant no. CYXZPT2025-08).

Availability of data and materials

The data generated in the present study may be requested from the corresponding author.

Authors' contributions

WH, YS, WZ and HX conceived and designed the study. WH and CY collected the data. WH, CY and YS contributed data or analysis tools. WH, CY and YZ performed the analysis. WH, WZ and HX wrote the manuscript. HX, WZ, WH and CY have checked and confirm the authenticity of all the raw data. All authors read and approved the final version of the manuscript.

Ethics approval and consent to participate

This study was conducted in accordance with the Declaration of Helsinki. The research protocol was approved by the Ethics Committee of the Second Hospital of Lanzhou University (approval no. 2023A-381) and informed consent was obtained from all patients and/or their legal guardians, as appropriate.

Patient consent for publication

Not applicable.

Competing interests

The authors declare that they have no competing interests.

References

1. Banales JM, Cardinale V, Carpino G, Marzioni M, Andersen JB, Invernizzi P, Lind GE, Folseraas T, Forbes SJ, Fouassier L, *et al*: Expert consensus document: Cholangiocarcinoma: Current knowledge and future perspectives consensus statement from the European network for the study of cholangiocarcinoma (ENS-CCA). Nat Rev Gastroenterol Hepatol 13: 261-280, 2016.
2. Ilyas SI and Gores GJ: Pathogenesis, diagnosis, and management of cholangiocarcinoma. Gastroenterology 145: 1215-1229, 2013.
3. Kendall T, Verheij J, Gaudio E, Evert M, Guido M, Goeppert B and Carpino G: Anatomical, histomorphological and molecular classification of cholangiocarcinoma. Liver Int 39 (Suppl 1): S7-S18, 2019.
4. Vij M, Puri Y, Rammohan A, G G, Rajalingam R, Kaliamoorthy I and Rela M: Pathological, molecular, and clinical characteristics of cholangiocarcinoma: A comprehensive review. World J Gastrointest Oncol 14: 607-627, 2022.
5. Nakeeb A, Pitt HA, Sohn TA, Coleman J, Abrams RA, Piantadosi S, Hruban RH, Lillemoe KD, Yeo CJ and Cameron JL: Cholangiocarcinoma. A spectrum of intrahepatic, perihilar, and distal tumors. Ann Surg 224: 463-73; discussion 473-5, 1996.

6. Khan SA, Tavolari S and Brandi G: Cholangiocarcinoma: Epidemiology and risk factors. Liver Int 39 (Suppl 1): S19-S31, 2019.
7. Everhart JE and Ruhl CE: Burden of digestive diseases in the united states part III: Liver, biliary tract, and pancreas. Gastroenterology 136: 1134-1144, 2009.
8. Banales JM, Marin JJG, Lamarca A, Rodrigues PM, Khan SA, Roberts LR, Cardinale V, Carpino G, Andersen JB, Braconi C, *et al*: Cholangiocarcinoma 2020: The next horizon in mechanisms and management. Nat Rev Gastroenterol Hepatol 17: 557-588, 2020.
9. Sato K, Zhang W, Safarikia S, Isidan A, Chen AM, Li P, Francis H, Kennedy L, Baiocchi L, Alvaro D, *et al*: Organoids and spheroids as models for studying cholestatic liver injury and cholangiocarcinoma. Hepatology 74: 491-502, 2021.
10. Yoshida GJ: Applications of patient-derived tumor xenograft models and tumor organoids. J Hematol Oncol 13: 4, 2020.
11. Drost J and Clevers H: Organoids in cancer research. Nat Rev Cancer 18: 407-418, 2018.
12. Invrea F, Rovito R, Torchiaro E, Petti C, Isella C and Medico E: Patient-derived xenografts (PDXs) as model systems for human cancer. Curr Opin Biotechnol 63: 151-156, 2020.
13. Miao X, Wang C, Chai C, Tang H, Hu J, Zhao Z, Luo W, Zhang H, Zhu K, Zhou W and Xu H: Establishment of gastric cancer organoid and its application in individualized therapy. Oncol Lett 24: 447, 2022.
14. Hughes CS, Postovit LM and Lajoie GA: Matrigel: A complex protein mixture required for optimal growth of cell culture. Proteomics 10: 1886-1890, 2010.
15. Broutier L, Mastrogiovanni G, Verstegen MM, Francies HE, Gavarró LM, Bradshaw CR, Allen GE, Arnes-Benito R, Sidorova O, Gaspersz MP, *et al*: Human primary liver cancer -derived organoid cultures for disease modelling and drug screening. Nat Med 23: 1424-1435, 2017.
16. Li L, Knutsdottir H, Hui K, Weiss MJ, He J, Philosophe B, Cameron AM, Wolfgang CL, Pawlik TM, Ghiaur G, *et al*: Human primary liver cancer organoids reveal intratumor and interpatient drug response heterogeneity. JCI Insight 4: e121490, 2019.
17. Li K, Liu C, Sui X, Li C, Zhang T, Zhao T, Zhang D, Wu H, Liu Y, Wang S, *et al*: An organoid co-culture model for probing systemic anti-tumor immunity in lung cancer. Cell Stem Cell 32: 1218-1234.e7, 2025.
18. Gong S, He K, Liu Y, Luo X, Ashraf K, He J, Li W, Yang L, Rehman TU, Shen M, *et al*: Scalable matrigel-free suspension culture for generating high-quality human liver ductal organoids. Cell Prolif 58: e70033, 2025.
19. Wijnakker JJAPM, Lim S, Schreurs R, Faria JF, Korving J, Begthel H, Iyer KK, Kouwer PHJ and Clevers H: Invasin-functionalized PIC hydrogels enable long-term 3D culture of epithelial organoids. Proc Natl Acad Sci USA 122: e2507500122, 2025.
20. Shamir ER and Ewald AJ: Three-dimensional organotypic culture: Experimental models of mammalian biology and disease. Nat Rev Mol Cell Biol 15: 647-664, 2014.
21. Lamarca A, Barriuso J, McNamara MG and Valle JW: Biliary tract cancer: State of the art and potential role of DNA damage repair. Cancer Treat Rev 70: 168-177, 2018.
22. Valle J, Wasan H, Palmer DH, Cunningham D, Anthoney A, Maraveyas A, Madhusudan S, Iveson T, Hughes S, Pereira SP, *et al*: Cisplatin plus gemcitabine versus gemcitabine for biliary tract cancer. N Engl J Med 362: 1273-1281, 2010.
23. Polak R, Zhang ET and Kuo CJ: Cancer organoids 2.0: Modelling the complexity of the tumour immune microenvironment. Nat Rev Cancer 24: 523-539, 2024.
24. Mu P, Zhou S, Lv T, Xia F, Shen L, Wan J, Wang Y, Zhang H, Cai S, Peng J, *et al*: Newly developed 3D in vitro models to study tumor-immune interaction. J Exp Clin Cancer Res 42: 81, 2023.
25. Linde N, Gutschalk CM, Hoffmann C, Yilmaz D and Mueller MM: Integrating macrophages into organotypic co-cultures: A 3D in vitro model to study tumor-associated macrophages. PLoS One 7: e40058, 2012.
26. Neal JT, Li X, Zhu J, Giangarra V, Grzeskowiak CL, Ju J, Liu IH, Chiou SH, Salahudeen AA, Smith AR, *et al*: Organoid modeling of the tumor immune microenvironment. Cell 175: 1972-1988. e16, 2018.